Asian Journal of Chemistry; Vol. 30, No. 2 (2018), 280-292

ASIAN JOURNAL OF CHEMISTRY

https://doi.org/10.14233/ajchem.2018.20889

Synthesis, Spectral, Thermal and Biological Studies of Some Metal Complexes Derived from Heterocyclic Mono Azo Dye Ligand 2'[(2'-Hydroxy-4-methyl phenyl)azo]imidazole

KHALID J. AL-ADILEE* and SAAD A. ATYHA

Department of Chemistry, College of Education, University of Al-Qadisiyah, Diwaniya 1753, Iraq

*Corresponding author: Tel: +964 7811596576; E-mail: khalid.jawad@qu.edu.iq; khalidke_1962@yahoo.com

Received: 23 June 2017; *Accepted*: 2 December 2017; *Published online*: 31 December 2017; AJC-18692

A new hetrocyclic mono azo dye ligand 2'[2'-(1-hydroxy-4-methyl phenyl)azo]imidazole (HMePAI) was prepared by reaction between diazonium chloride salt solution of 2'-amino-4-methyl phenol with imidazole in alkaline ethanolic solution. Nine metal complexes with Cr(III), Mn(II), Fe(III), Co(III), Ni(II), Cu(II), Zn(II), Cd(II) and Hg(II) ions were prepared and characterized by analytical and spectral techniques like elemental analysis (CHN), metal contents, molar conductance, magnetic moments, ^{1}H NMR, Mass spectra, infrared, electronic spectral, XRD spectra, SEM and thermal studies (TGA & DSC). The results indicated that the ligand (HMePAI) behaves as a tridentate in case of 1:2 [metal:ligand] complexes. Investigation of the stereochemistry of metal complexes have octahedral geometry. Biological activity of ligand (HMePAI) and its metal complexes against two types of bacteria, *Staphylococcus aureus* (Gram-positive) and *Escherichia coli* (Gram-negative) by agar plate different technique. The biological activity was also conducted by cells viability and cytotoxicity assay on ligand and Ni(II) complex by using the lines of cancerous liver cells of the type HEPG2 and compared with line of the ordinary cells.

Keywords: Azo imidazole, Metal complexes, Synthesis and Characterization, Biological activity.

INTRODUCTION

Azo imidazole dyes have enormous applications in different fields such as polymerization [1], textile [2], leather paper, paint, wood, silk, rubber, plastics, cosmetics operations and coating industries as a dyeing agent [3-6]. It is also used in the pharmaceutical and food industries as a colouring agent [7]. Imidazole ring is an important pharmacophore in drug discovery. Extensive biochemical and pharmacological studies have confirmed that imidazole molecule is associated with a wide range of biological activities including anticancer [8,9], antibacterial [10], antifungal [11], antioxidant [12], antihypertensive [13] and anticoagulant [14], properties. In recent years, there have been important applications of azo dye was permeate into the field of electronic industry as a strong components in the DVD-R (digital versatile disc-recordable) because of its characteristic as stable metal azo dyes. Azo dyes can be coated easily by spin coating method which increases good thermal stability, refractive index [15] and also metal complexes of the azo dyes are having extensive application in electro-photographic toners as charge controlling agents, developers in powder coating materials, electric materials and in electrostatic separation processes, in-ink jets and in colour filters [16-18]. The dyeing ability of the azo dyes depends on the functional group present in the azo dyes compounds, such as hydroxyl, carboxylic acid, halogens, esters and amines [19,20]. An important uses of azo imidazole compounds used analytical reagents for solvent extraction to determination of some metal ions [21,22]. The heterocyclic azo imidazole compounds have important role in spectral determination field to determine the trace amount of elements especially transition metal ions and heavy metals because of high sensitivity and selectivity [23,24].

The present work describes the synthesis and spectral characterizations of 2'[2'-(1-hydroxy-4-methyl phenyl)azo]-imidazole (HMePAI = HL), containing phenolic-OH function and imidazole moiety. The heterocyclic mono azo dye ligand and its metal complexes were studied by various spectral analysis and screened for their biological activities. As well as the study of ligand and Ni(II) complex of prescription drug anticancer by using the lines of cancerous liver cells of the type HePG2 and compared with line of the ordinary cells.

EXPERIMENTAL

All other organic chemicals, solvents and inorganic salts were available from multiple companies, Fluka, B.D.H, Merck, Scharin, Sigma and Alderich and used without further purification.

Microanalytical data (CHN) were collected on EA 300 CHNS Elemental analyzer. Mass spectra were recorded on a Shimadzu Agilent Technologies 5973 at 70 and MSD energy using a direct insertion probe (Acq method 10 W energy) at 90-110 °C. ^{1}H NMR spectra were recorded using a Bruker 400 MHz spectrophotometer in DMSO-d_6 using TMS as an internal reference. Infrared spectra were taken on Shimadzu 8400 S FT-IR spectrophotometer with samples prepared as KBr pellets. Electronic spectral studies were performed on UV-visible. T80-PG spectrophotometer in absolute ethanol (10^{-3} M) in the range (200-1100) nm. The metal contents were determined by using atomic absorption technique by Shimadzu AA-6300. TGA, DSC and DTG analysis were measured with England PL-TG using Rheometric scientific TGA-1000. SEM images were taken using micrograph kyky 3200. X-ray diffraction was measured using Bestec Germany Alminium anode model X-pertpro, wavelength of X-ray beam (Cu K_α) 1.54 Å, Anode material = Cu, the Voltage = 40 KV and current = 30 mA. Molar conductivity measurements were recorded on conductivity bridge model 31A in dry DMF (10^{-3} M) solution at room temperature. Magnetic susceptibility for prepared metal complexes was measured on a Burker Magnet (BM) and the diamagnetic correction was made by Pascal's constants at room temperature by using faraday method. The pH of solutions was measured on a Philips pw 9421 pH meter (± 0.001). The chloride ion contents in Cr(III), Fe(III) and Co(III) complexes determined as per Vogel's procedure [25] and $AgNO_3$ solution.

Synthesis of 2'[2'-(1-hydroxy-4-methyl phenyl)azo]-imidazole (HL): The new mono heterocyclic azo dye ligand (HMePAI) (**Scheme-I**) has been synthesized by the diazotization coupling by flowing method proposed by Al-Adilee *et al.* [24,26] with some modification. 2'-Amino-4-metheyl phenol (1.23 g, 0.01 mol) was dissolved in 4 mL conc. HCl and 25 mL distilled water and cooled to 0 °C sodium nitrite (0.75 g, 0.01 mol) was dissolved in 20 mL distilled water and cooled to 0-5 °C. The diazotized solution was added drop-wise with constant stirring to imidazole (0.68 g, 0.01 mol) dissolved in 100 mL ethanol and 18 mL of 7 % sodium hydroxide with cooling and stirring continuously for 1 h at 0-3 °C in ice-bath and allowed to stand overnight and acidified with dilute HCl to pH = 6.0. The precipitate was filtered off and washed several times with cold distilled water and recrystallized twice from hot ethanol and then dried in oven at 50 °C for several hours and stored in a desiccator over anhydrous $CaCl_2$. The yield was 81 % of dark red crystals and melting point found to be 130 °C. The purity was confirmed by the elemental analysis and TLC techniques.

Synthesis of metal complexes: The metal complexes were prepared using corresponding metal chlorides and azo dye ligand (HMePAI) at 1:2 [M:L] molar ratio. An ethanolic solution (0.404 g, 0.002 mol) was dissolved in 50 mL of azo dye ligand and (0.001 mol) of Cr(III), Mn(II), Fe(III), Co(III), Ni(II), Cu(II), Zn(II), Cd(II) and Hg(II) chlorides dissolved in 40 mL hot buffer solution (ammonium acetate) at pH = 7.0 for each metal ions was refluxed on water bath for 1-2 h. The separated solid metal complexes were filtered off, washed with little warm ethanol (5 mL) to remove any traces of unreacted material and wished with distilled water. The metal complexes obtained were finally dried in oven at 60 °C to several hours and kept under vacuum desiccators over fused $CaCl_2$. The % yield, m.p., molecular formula, m.w., colour and element analysis data (CHN) of azo dye ligand and its metal complexes are collected in Table-1.

RESULTS AND DISCUSSION

Characterization of azo dye ligand and its metal complexes: The mono heterocyclic azo dye ligand (HMePAI) was dark red crystals but the metal complexes of this ligand vary in colour depending on metal ions. The experimental result of the elemental analysis of the prepared azo dye ligand and its metal complexes are in good agreement with theoretical expec-

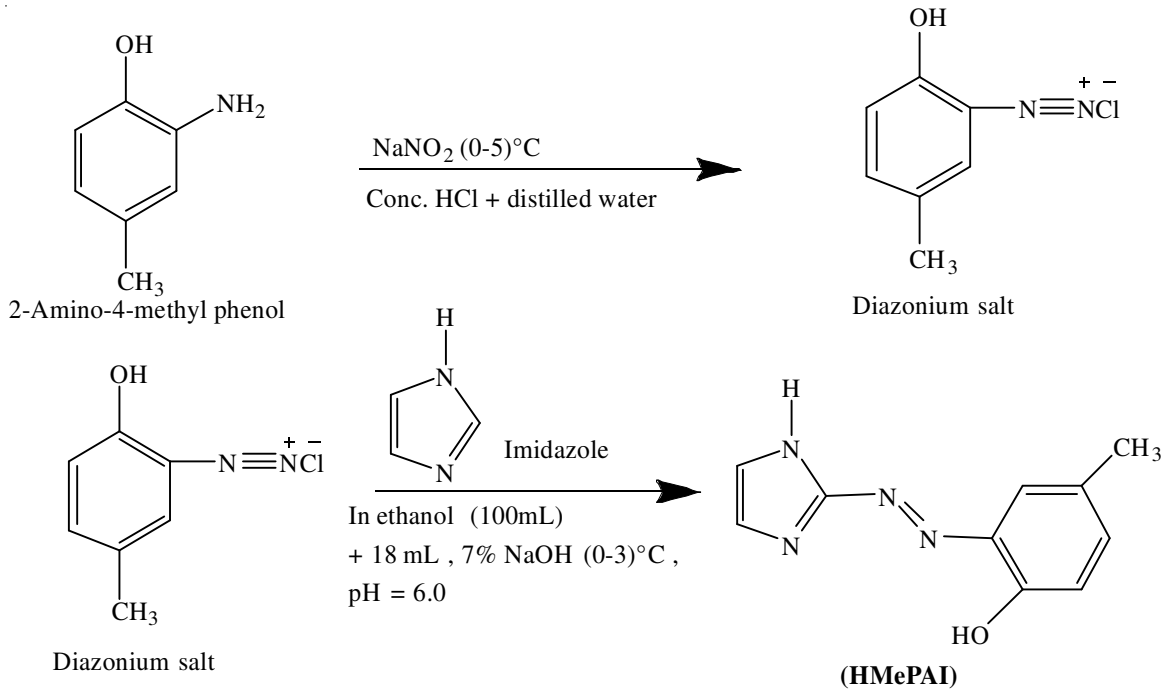

Scheme-I: Syntheic pathway of heterocyclic azo dye ligand 2'[2'-(1-hydroxy-4-methyl phenyl)azo]imidazole (HMePAI = HL)

TABLE-1
ANALYTICAL AND PHYSICAL DATA OF AZO DYE LIGAND AND ITS METAL COMPLEXES

Compound	Colour	m.p. (°C)	Yield (%)	m.f. (m.w.)	Elemental analysis (%): Found (calcd.)			
					C	H	N	M
HMePAI	Dark red	130	81	$C_{10}H_{10}N_4O$ (202.21)	59.18 (59.40)	4.91 (4.98)	27.13 (27.71)	–
$[Cr(L)_2]Cl$	Dark brown	192	78	$C_{20}H_{18}N_8O_2CrCl$ (489.86)	49.23 (49.04)	3.59 (3.70)	23.22 (22.87)	10.89 (10.61)
$[Mn(L)_2]$	Redish orange	198	63	$C_{20}H_{18}N_8O_2Mn$ (457.35)	52.12 (52.52)	4.05 (3.97)	24.95 (24.50)	12.23 (12.01)
$[Fe(L)_2]Cl$	Brown	185	67	$C_{20}H_{18}N_8O_2FeCl$ 493.71)	48.88 (48.65)	3.58 (3.67)	22.93 (22.69)	11.65 (11.31)
$[Co(L)_2]Cl$	Dark purple	193	74	$C_{20}H_{18}N_8O_2CoCl$ (496.80)	50.71 (50.38)	3.67 (3.80)	23.67 (23.50)	12.48 (12.36)
$[Ni(L)_2]$	Olive	201	71	$C_{20}H_{18}N_8O_2Ni$ (461.11)	52.55 (52.09)	4.02 (3.93)	24.37 (24.30)	13.71 (12.73)
$[Cu(L)_2]$	Dark green	195	82	$C_{20}H_{18}N_8O_2Cu$ (465.96)	51.72 (51.55)	3.77 (3.89)	24.38 (24.05)	14.07 (13.64)
$[Zn(L)_2]$	Brown	205	86	$C_{20}H_{18}N_8O_2Zn$ (467.82)	51.59 (51.35)	3.93 (3.88)	24.10 23.95	14.19 (13.98)
$[Cd(L)_2]$	Redish purple	210	66	$C_{20}H_{18}N_8O_2Cd$ (514.82)	46.47 (46.66)	3.42 (3.52)	21.85 (21.76)	–
$[Hg(L)_2]$	Redish brown	200	79	$C_{20}H_{18}N_8O_2Hg$ (603.00)	40.36 (39.84)	3.07 (3.01)	18.83 (18.58	–

tations. The monoazo dye ligand and its metal complexes were soluble in most organic solvents such as methanol, ethanol, acetone, chloroform, pyridine, DMF and DMSO giving stable solutions at room temperature but in soluble in water. However, some physical and analytical data are given in Table-1.

Metal:Ligand ratio: The possible structural formula of prepared metal complexes was studied by molar ratio method at pH = 7.0 and optimum concentration at wavelength maximum absorption (λ_{max}). The solutions of metal complexes increase the intensity of the colours as an approach point of intersection ratio [M:L] and colour continous constant at passing this point which indicates that the metal complexes formed in constant of solution. The metal:ligand [M:L] ratio in all metal complexes was found to form 1:2 chelates. These results are in agreement with values reported for some aryl azo imidazole complexes [24,27].

Molar conductivity measurements: The molar conductance measurements of the prepared metal complexes were measured in the solvent DMF (10^{-3} M) at room temperature are shown in Table-2. The high values of molar conductivity of the Cr(III), Fe(III) and Co(III) complexes indicate that complexes are 1:1 electrolyte with ionic nature but the low values of molar conductivity of metal complexes of Mn(II), Ni(II), Cu(II), Zn(II), Cd(II) and Hg(II) ions indicate that non-electrolytic nature and no chloride ions are present outside the coordination spheres [28,29].

Calculation stability constants: The stability constants (β and log β) of metal complexes were obtained spectrophotometrically by measuring the absorbance of solution mixture of azo dye ligand and metal ion at pH = 7.0 and optimum concentration at fixed wavelength (λ_{max}). The degree formation of the metal complexes is calculated according to the relationship, $\beta = (1-\alpha)/4\alpha^3c^2$, $\alpha = (A_m-A_s/A_m)$, where A_s and A_m are the absorbance of the partially and fully formed complexes respectively. The stability constants of metal complexes according to the following sequence:

Mn(II) > Ni(II) > Fe(III) > Zn(II) > Co(III) > Cr(III) > Hg(II) > Cd(II) > Cu(II).

The sequence of metal ions of the first row transition metal with Irving-Williams series of stability constant [30,31].

^{1}H NMR spectra: ^{1}H NMR spectra of mono azo dye ligand (HMePAI) and Ni(II) complex was measured in DMSO-d_6 as solvent with TMS as an internal reference (400 MHz) and characterized by presence of a low-field. ^{1}H NMR spectrum of azo dye ligand shows a signal at δ = 12.164 ppm (S, 1H) due to the presence of OH-group, a signal at δ = 10.234 ppm (S, 1H) due to the presence of amide (NH) in imidazole ring and a signal at δ = 9.623 ppm (S, 4H and 5H) protons due to imidazole ring. A signal at δ = 7.864 ppm (d, 3H, 5H) and a signal at δ = 7.123 ppm (q, 6H) due to the presence of aromatic protons. The signal at δ = 2.505-2.513 ppm (S, 3H) due to the presence of CH_3 group. While a signal at δ = 1.151-1.238 ppm (S) due to solvent protons [32,33].

The ^{1}H NMR spectrum of Ni(II) complex shows a signal at δ = 10.046 ppm (S, 1H) due to the presence of amide (NH) proton in imidazole molecule while a signal at δ = 10.023 ppm (S, 4H and 5H) proton due to imidazole ring. A signal at δ = 7.69-7.731 ppm (m, 3H, 5H) and a signal at δ = 6.924 ppm (S, 6H) due to the presence of aromatic protons. The signal at δ =

TABLE-2
MOLAR CONDUCTIVITY, STABILITY CONSTANTS VALUES (β AND log β), OPTIMAL CONCENTRATION, MAXIMUM WAVELENGTH (λ_{max}) AND MOLAR ABSORPTIVITY (ε) OF METAL COMPLEXES

Ligand (HMePAI)	Metal ion	Optimal conc. $\times 10^{-4}$ M	Maximum wavelength (λ_{max}, nm)	Molar absorptivity (ε) $\times 10^3$ L mol^{-1} cm^{-1}	Molar conductivity (S cm^2 mol^{-1})	Stability constant (β) (L^2 mol^{-2})	log β
Ligand = HL (HMePAI) λ_{max} = 431 nm $\varepsilon = 2.84 \times 10^3$ L mol^{-1} cm^{-1} Conc. = 1.75×10^{-4} M	Cr(III)	2.00	480	9.61	78.21	12.66×10^8	9.10
	Mn(II)	1.50	447	7.78	12.28	33.30×10^8	9.52
	Fe(III)	2.25	472	6.67	68.59	19.56×10^8	9.30
	Co(III)	1.75	505	10.55	71.09	18.15×10^8	9.26
	Ni(II)	1.50	635	3.45	11.84	24.20×10^8	9.38
	Cu(II)	2.00	665	1.03	12.17	6.15×10^8	8.79
	Zn(II)	1.50	476	9.11	14.66	19.50×10^8	9.29
	Cd(II)	1.50	450	1.66	10.86	8.51×10^8	8.93
	Hg(II)	1.75	475	9.79	12.43	9.81×10^8	8.99

2.509-2.678 ppm (S, 3H) due to the presence of CH_3 group and a signal at δ = 1.233-1.283 ppm (S) due to the solvent.

The signal of proton (-OH group) disappearance in spectrum of Ni(II) complex indicates hydrogen atom of –OH group replacement by Ni(II) ion during coordination with azo dye ligand [34,35].

Mass spectra of mono azo dye ligand and its Ni(II) complex: The mass spectra of mono azo dye ligand (HMePAI) and Ni(II) complex and data fragmentation have been studied as stated in the literature [25,32,34,36].

The mass spectrum of the azo dye ligand (Fig. 1, **Scheme-II**) shows a final peak at m/z^+ = 201.9 corresponding to the azo dye ligand (HMePAI) $[C_{10}H_{10}N_4O]$ (atomic mass 202.22). Other peaks like at m/z^+ = 199.9 due to loss of 2H protons, $[C_{10}H_8N_4O]^+$ ion while peak at m/z^+ = 171.1 corresponding to $[C_9H_7N_4]^+$ ion due to loss methyl group (-CH_3) and oxygen atom. The loss of azo group (-N=N-) give peak at m/z^+ = 143.2 is due to $[C_9H_7N_2]^+$ ion. The peaks at m/z^+ = 68.1 and m/z^+ = 40.1 due to imidazole ring, $[C_3H_4N_2]$ and $[C_3H_4]$ respectively. Other peaks like m/z^+ = 77.2 and 53.1 correspond to $[C_6H_5]^+$and $[C_4H_5]^+$ fragments.

The mass spectrum of the Ni(II) complex (Fig. 2, **Scheme-III**) showed a molecular ion peak M^+ at m/z^+ = 461.5 corresponding to the Ni(II) complex, $[C_{20}H_{18}N_8O_2]$, (atomic mass 461.35), equivalent to its molecular weight supporting the suggested structure for the Ni(II) complex. The Ni(II) complex gives peak at m/z^+ = 259.6 is attributed to $[C_{10}H_9N_4ONi]^+$because of loss $[C_{10}H_9N_4O]^+$. The peak at m/z^+ = 201.1 corresponding to

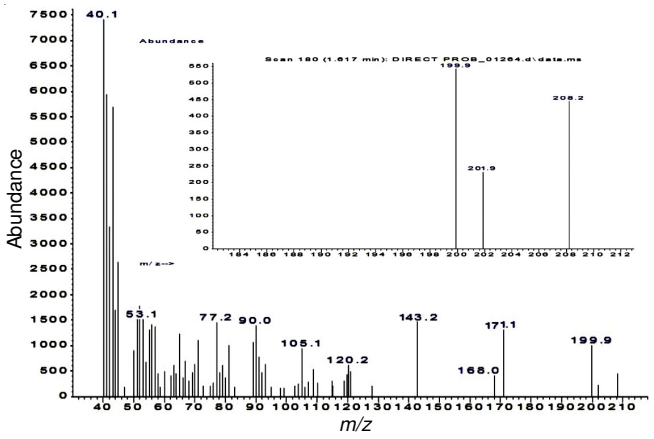

Fig. 1. Mass spectrum of azo dye ligand (HMePAI)

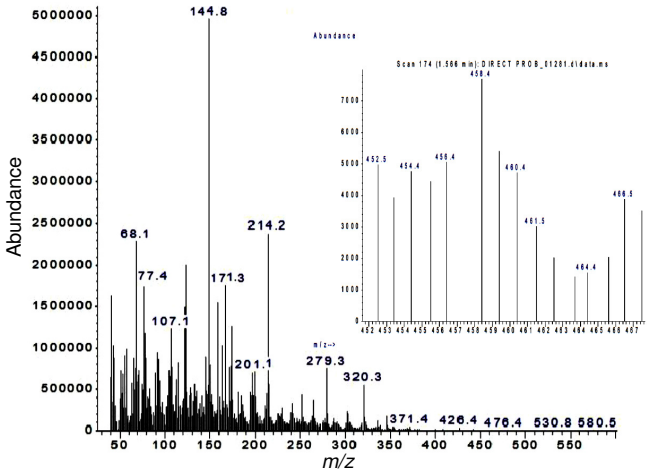

Fig. 2. Mass spectrum of Ni(II) complex; $[Ni(L)_2]$

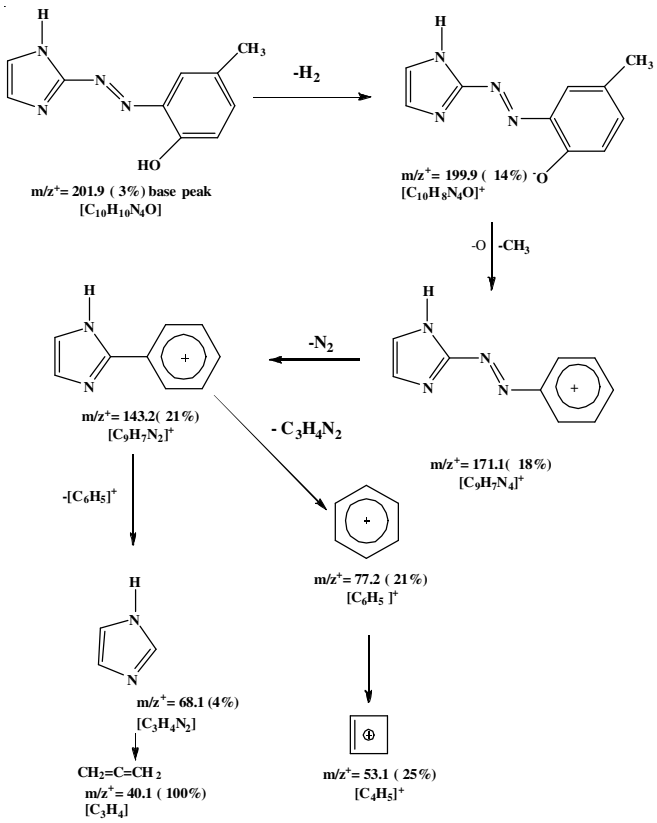

Scheme-II: Mass spectrum fragmentation of mono azo dye ligand (HMePAI)

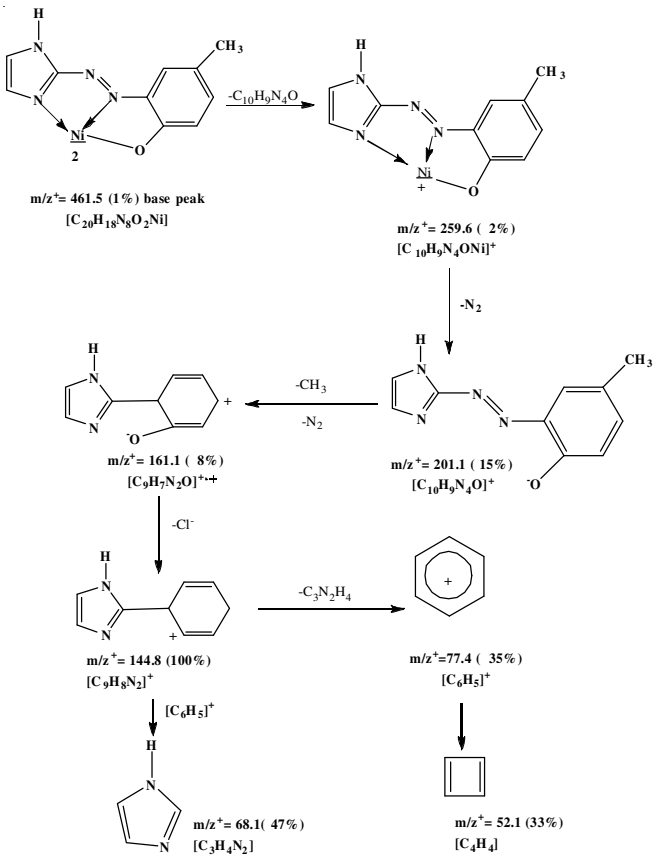

Scheme-III: Mass spectrum fragmentation of Ni complex; $[Ni(L)_2]$

$[C_{10}H_9N4O]^+$ion due to loss nickel ion, while the peak at m/z^+ = 161.1 due to $[C_9H_7N_2O]^+$ attributed to loss methyl group (-CH_3) and azo group (-N=N-). Other peaks like m/z^+ = 144.8, 68.1, 77.4 and 52.1 Correspond to $[C_9H_8N_2]^+[C_3H_4N_2]$, $[C_6H_5]^+$ and $[C_4H_4]$ respectively. The intensity of these peaks gives the idea of the stability of fragments.

Infrared spectra: Infrared spectral data of the prepared mono azo dye ligand (HMePAI) and its Cr(III), Mn(II), Fe(III), Co(III), Ni(II), Cu(II), Zn(II), Cd(II) and Hg(II) complexes are presented in Table-3. The IR spectrum of the free azo dye ligand showed a weak and broad band around 3420 cm^{-1} which is assigned to ν(-OH) group in the ligand which is absent in all metal complexes showing the deprotonation of the azo dye ligand and coordination with metal ion [24]. The medium band observed at 3181 cm^{-1} in the free ligand was attributed to ν(N-H) stretching vibration of the imidazole moiety [37]. The position of this band remained at nearly the same frequency in spectra of the metal complexes, which may be explained by nonparticipation in complex. The weak bands at 3080 and 2961 cm^{-1} in the spectrum of free ligand which is due to ν(C-H) aromatic and aliphatic respectively. These bands are stable in position as well as intensity in both free ligand and all metal complexes. The strong band at 1645 cm^{-1} in the free ligand was attributed to ν(C=N) of the imidazole ring (N_3). This band shifts to lower wave number side (1542, 1605) cm^{-1} in all metal complexes indicating the coordination [24,33]. The sharp band at 1468 cm^{-1} is characteristic of the azo group ν(-N=N-) in the free ligand. This band shifted to a lower wave number side in all metal complexes in this frequency to 1458-1450 cm^{-1} indicates the participation of the azo group nitrogen (N_3) in coordination with metal ions [34,38].

The far IR spectra of the metal complexes exhibited new band that are not present in the azo dye ligand. These bands are located at (578 and 562) cm^{-1} and (480 and 432) cm^{-1} due to ν(M-O) and ν(M-N) respectively [24,39]. IR spectral data lead to suggest that the azo dye ligand (HMePAI) behaves as ionic tridentate chelating agent and coordination with metal ion by using sites are the nitrogen atom of the heterocyclic imidazole ring (N_3), nitrogen atom of azo group nearest to a phenyl ring (N_3) and a phenolic oxygen to forming two five membered chelating agent.

Electronic spectral studies: The electronic absorption spectra of the azo dye ligand (HMePAI) and its metal complexes were recorded in absolute ethanol (10^{-3} M) in the UV-visible region (200-1100) nm at room temperature. The spectral data and the magnetic moment of prepared metal complexes are presented in Table-4.

The electronic spectrum of free ligand shows three bands at 222 nm (45045 cm^{-1}), 247 nm (40485 cm^{-1}) due to π→π* and 431 nm (23202 cm^{-1}) may be assigned n→π* charge transfer transition due to presence conjugation in the imidazole ring [33,40].The electronic spectrum of the Cr(III) complex displayed bands at 240 nm (41667 cm^{-1}) and 480 nm (20833 cm^{-1}). These two bands are assignable to center ligand and $^4A_2g \rightarrow {}^4T_1g_{(F)}$ transitions respectively in an octahedral environment [24,34].

The Mn(II) complex exhibited three bands, at 250 nm (40000 cm^{-1}), 295 nm (33898 cm^{-1}) and 447 nm (22371 cm^{-1}) a assignable to center ligand, $^2A_1g \rightarrow {}^4T_1g_{(G)}$ and $^2A_1g \rightarrow {}^4T_1g_{(P)}$ transitions, respectively in an octahedral environment [24,34,41]. The electronic absorption spectrum of the Fe(III) complex exhibited three absorption bands at 254 nm (39370 cm^{-1}), 312 nm (32051 cm^{-1}) and 472 nm (21186 cm^{-1}) due to center ligand, $^2A_1g \rightarrow {}^2T_1g_{(G)}$ and $^2A_1g \rightarrow {}^2T_1g_{(P)}$ transitions respectively in an octahedral geometry [28,33,42]. The electronic spectrum of the Co(III) complex exhibited four absorption bands, the first and second bands at 256 nm (39063 cm^{-1}) and 297 nm (33670 cm^{-1}) which may be attributed to center ligand transitions while the third and four bands located at 505 nm (19802 cm^{-1}) and 970 nm (10309 cm^{-1}) assignable to $^1A_1g \rightarrow {}^1T_2g_{(F)}$ and $^1A_1g \rightarrow {}^1T_1g_{(P)}$ transitions respectively in an octahedral geometry [34,35,43]. The Ni(II) complex exhibited three spin-allowed absorption bands at 975 nm (10256 cm^{-1}), 635 nm (15748 cm^{-1}) and 475 nm (21053 cm^{-1}) which may be attributed to $^3A_2g \rightarrow {}^3T_2g_{(F)}$, $^3A_2g \rightarrow {}^3T_1g_{(F)}$ and $^3A_2g \rightarrow {}^3T_1g_{(P)}$ transitions respectively, while the band at 256 nm (39062 cm^{-1}) due to center ligand and the shape of this complex in an octahedral geometry [44]. The dark green coloured Cu(II) complex exhibited a single broad asymmetric band in the region 665 nm (15038 cm^{-1}). The broadness of the band indicates the three transitions $^2B_1g \rightarrow {}^2A_1g_{(u1)}$, $^2B_1g \rightarrow {}^2B_2g_{(u2)}$ and $^2B_1g \rightarrow {}^2Eg_{(u3)}$, which are of similar energy and give rise to only one broad absorption band ($^2B_1g \rightarrow {}^2Eg$). The broadness of the band may be due to dynamic Jahn-Teller distortion [7,24,33,34]. All of these data suggested a distorted octahedral geometry around Cu(II)complex ion (Z-in or Z-out).

The Zn(II), Cd(II) and Hg(II) complexes do not show any *d-d* transition because of saturated with electrons (d^{10}). The absorption bands at longer wavelength 476 nm (21008 cm^{-1}),

TABLE-3
INFRARED SPECTRAL DATA (cm^{-1}) OF AZO DYE LIGAND AND ITS METAL COMPLEXES (KBr DISC)

Group	HMePAI	Cr(III)	Mn(II)	Fe(III)	Co(III)	Ni(II)	Cu(II)	Zn(II)	Cd(II)	Hg(II)
ν(OH)	3420w,br	–	–	–	–	–	–	–	–	–
ν(N-H)	3181m	3282s	3278m	3363m,br	3341m,br	3356m,br	3340s	3340w,br	3348m,br	3248m
ν(C=N) Imd.	1645vs	1565m	1542m	1604w	1605w	1542w	1604w	1602w	1601w	1568w
ν(C=C)	1542vs	1510s	1512s	1518s	1504s	1515s	1515s	1518s	1515s	1518m
ν(N=N)	1480m	1450m	1458w	1458w	1458w	1458w	1454w	1450w	1450w	1458w
ν(C-N=N-C)	1278w, 750m	1245m, 663w	1281w, 633m	1250w, 638w	1249w, 671w	1234w, 671s	1250w, 670w	1249w, 675w	1249w, 663w	1249w, 671w
ν(Benz. R. Deff.)	1110m	1110w	1118w	1134w	1110w	1111w	1134m	1118w	1119w	1110w
ν(Imi- R. Deff.)	810m	810s	818s	817s	818s	818s	818s	817m	818s	810s
ν(M-O)	–	570w	571w	563w	562w	573w	572w	572w	578w	571w
ν(M-N)	–	465w	455w	432w	462w	465w	480w	464w	438w	472w

TABLE-4
ELECTRONIC SPECTRA (nm, cm^{-1}), MAGNETIC MOMENTS, PROPOSED STRUCTURE AND HYBRIDIZATION OF METAL COMPLEXES

Compounds	λ_{max} (nm)	Absorption bands (cm^{-1})	Transitions	μ_{eff} (BM)	Geometry	Hybridization
Ligand = HL (HMePAI)	222	45045	$\pi \rightarrow \pi^*$	–	–	–
	247	40485	$\pi \rightarrow \pi^*$			
	431	23202	$n \rightarrow \pi^*$			
$[Cr(L)_2]Cl$	240	41667	Center ligand	3.61	Octahedral (Regular)	d^2sp^3
	480	20833	$^4A_2g \rightarrow {}^4T_1g_{(F)}$			
$[Mn(L)_2]$	250	40000	Center ligand	1.81	Octahedral (Distorted) (Z-out)	d^2sp^3 (Low spin)
	295	33898	$^2A_1g \rightarrow {}^4T_1g_{(G)}$			
	447	22371	$^2A_1g \rightarrow {}^4T_1g_{(P)}$			
$[Fe(L)_2]$ Cl	254	39370	Center ligand	1.78	Octahedral (Distorted) (Z-out)	d^2sp^3 (Low spin)
	312	32051	$^2A_1g \rightarrow {}^2T_1g_{(G)}$			
	472	21186	$^2A_1g \rightarrow {}^2T_1g_{(P)}$			
$[Co(L)_2]$ Cl	256	39063	Center ligand	Diamag.	Octahedral (Regular)	d^2sp^3 (Low spin)
	297	33670	Center ligand			
	505	19802	$^1A_1g \rightarrow {}^1T_2g_{(F)}$			
	970	10309	$^1A_1g \rightarrow {}^1T_1g_{(F)}$			
$[Ni(L)_2]$	475	21053	$^3A_2g \rightarrow {}^3T_1g_{(P)}$	3.08	Octahedral (Regular)	sp^3d^2 (High spin)
	635	15748	$^3A_2g \rightarrow {}^3T_1g_{(F)}$			
	975	10256	$^3A_2g \rightarrow {}^3T_2g_{(F)}$			
$[Cu(L)_2]$	665	15038	$^2B_1g \rightarrow {}^2Eg$	1.78	Octahedral (distorted) (Z-in or Z-out)	sp^3d^2
$[Zn(L)_2]$	476	21008	$d\pi (Zn)^{+2} \rightarrow \pi^*(L)$	Diamag.	Octahedral (Regular)	sp^3d^2
$[Cd(L)_2]$	452	22124	$d\pi (Cd)^{+2} \rightarrow \pi^*(L)$	Diamag.	Octahedral (Regular)	sp^3d^2
$[Hg(L)_2]$	479	20877	$d\pi (Hg)^{+2} \rightarrow \pi^*(L)$	Diamag.	Octahedral (Regular)	sp^3d^2

452 nm (22124 cm^{-1}) and 479 nm (20877 cm^{-1}) assignable to M→π* (ligand) charge transfer transitions and in an octahedral environment [27,29,45]. The UV-visible spectra of azo dye ligand (HMePAI) and some metal complexes are shown in Fig. 3.

Magnetic studies: The magnetic moment value of Cr(III) complex is 3.61 BM, this value is too close to the theoretical magnetic moment for the Cr(III) ion (μ_{eff} = 3.87 BM) due to presence of three electrons unpaired (t_2g^3 eg^0), which may suggest a regular structure and d^2sp^3 hybridization [24,46]. The Mn(II) complex exhibited the magnetic moment value of 1.81 BM which indicates distorted octahedral geometry (Z-out) due to presence of one electron unpaired (t_2g^5 eg^0, low spin) because of strong ligand and d^2sp^3 hybridization [24,28,33]. The magnetic moment value of the Fe(III) complex is 1.78 BM due to presence of one electron unpaired (t_2g^5 eg^0) which may suggest distorted octahedral geometry (Z-out, low spin) and d^2sp^3 hybridization [28,33,47]. The Co(II) complex was found to be diamagnetic indicates the low spin behaviour because of that Co(II) ion which is oxidized to Co(III) ion during complexation in aqueous solution with presence of strong ligand such as azo imidazole ligands which may suggest a regular geometry (t_2g^6 eg^0) and d^2sp^3 hybridization [48,49]. The magnetic moment value of the Ni(II)complex is 3.08 BM within the range of 2.8-3.5 BM because of two electrons unpaired which may suggest a regular octahedral structure (t_2g^6 eg^2, high spin) and sp^3d^2 hybridization [44,50]. The Cu(II) complex showed magnetic moment of (1.78) BM is slightly higher than the spin-only value of (1.73) BM expected for one electron unpaired which offers the possibility of an distorted octahedral geometry, (t_2g^6 eg^3) and sp^3d^2 hybridization for these metal complexes [32,35,51]. The magnetic moment values of Zn(II), Cd(II) and Hg(II) complexes are diamagnetic consistent with the d^{10} (t_2g^6 eg^4) configuration which indicates an octahedral geometry and sp^3d^2 hybridization [52,53].

According to these results, the structural formula of prepared metal complexes in this work may be proposed in Fig. 4.

Thermal studies: The ligand and its metal complexes have thermal properties are examined from ambient temperature up to 700 °C in nitrogen atmosphere [54,55]. The results of thermogravimetry of ligand and metals complexes are listed in Table-5.

X-ray diffraction study (XRD): In this work, we studied the crystalline structure of prepared ligand (HMePAI) and its metal complexes in solid state by using X-rays diffractometer in the range of 2θ = 0-80° value. It is observed that ligand contained several sharp peaks which indicate the crystalline nature, while the metal complexes were different in nature where observed the Cr(III), Fe(III) and Cd(II) metal complexes contained rate the crystalline nature more than the amorphous nature because the sharp peaks are more than broad peaks while observed in Mn(II), Cu(II) and Zn(II) metal complexes contained rate the crystalline nature nearly equal the amorphous nature because the sharp peaks nearly equal broad peaks while observed in the Co(III), Ni(II) and Hg(II) metal complexes contained rate the crystalline nature less than the amorphous nature because the sharp peaks are less than broad peaks [56,57]. To calculate d-spacing or d values of reflections were obtained using Braggs equation $n\lambda = 2d \sin\theta$, where d is the spacing between the crystalline levels, n is an integer (1,2,3….), λ is the wavelength of X-ray CuK_α = 1.540598 Å, θ is the diffraction angle and the values of d and associated data depict the 2θ value of each peak, relative intensity also the particle size distribution histogram for ligand and metal complexes are listed

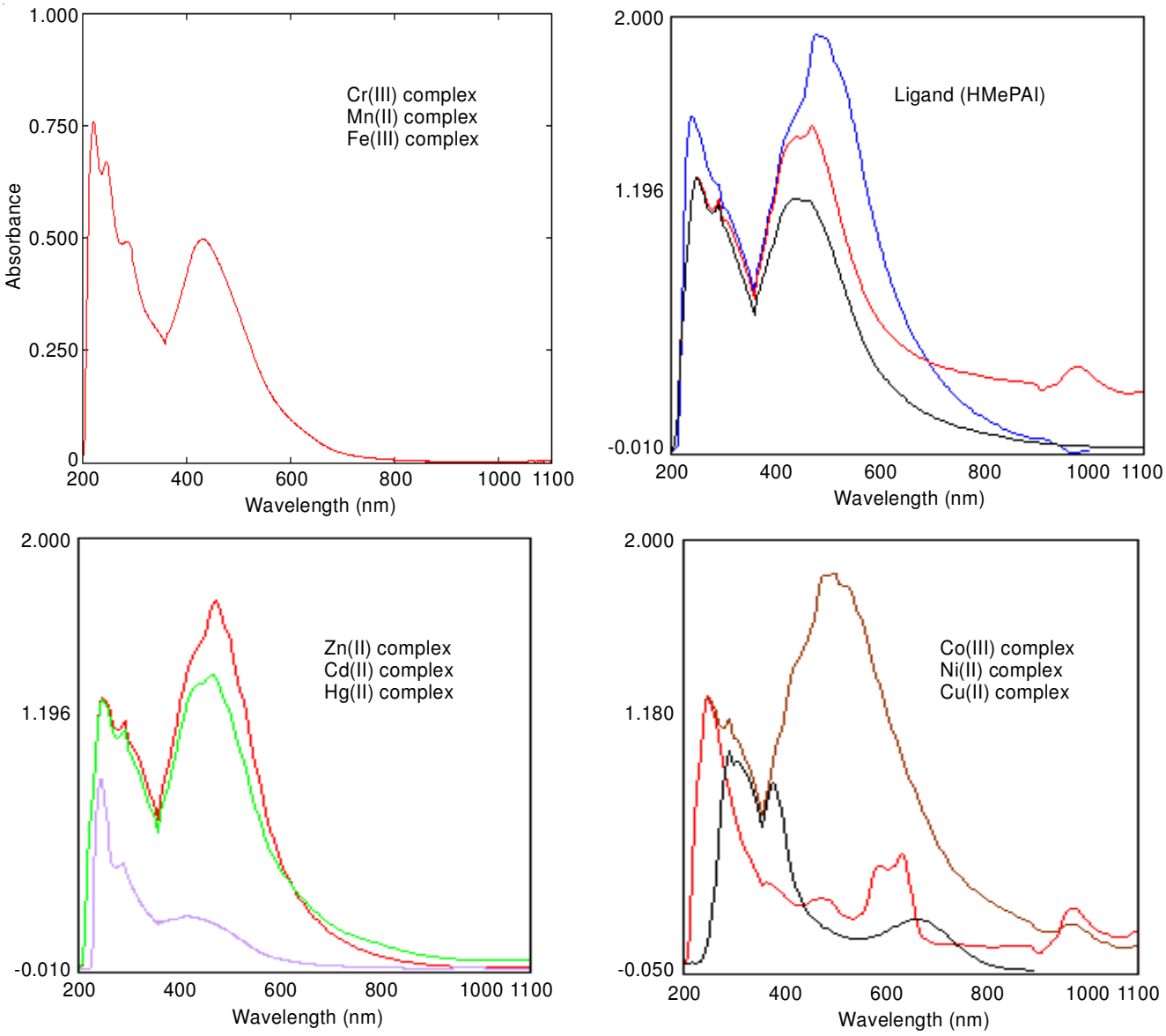

Fig. 3. UV-visible spectra of azo dye ligand (HMePAI) and its metal complexes

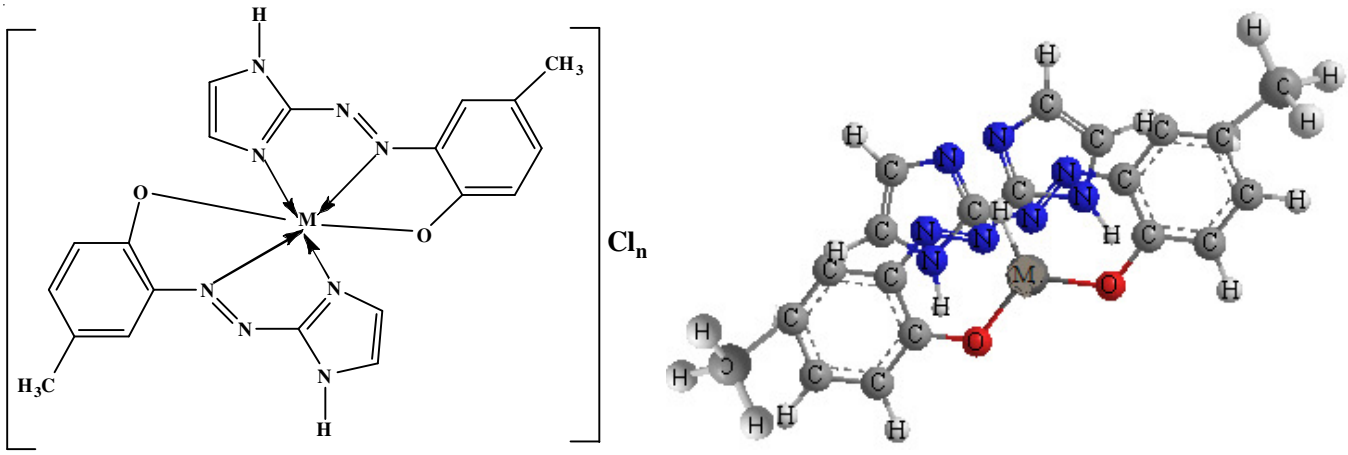

Fig. 4. Proposed structural formula of chelate metal complexes

in Table-6. The XRD peak shift to lower angle in metal complexes because of increased of *d*-spacing in the complexes and the average size of the particles and their size distribution were evaluated by the Scherer equation, $D = k\lambda/\beta\cos\theta$, where D is the average grain size, k is Blanks constant (0.891), λ is the X-ray wavelength (0.15405 nm) and θ and β are the diffraction

TABLE-5
THERMAL ANALYSIS OF AZO DYE LIGAND (HMePAI) AND ITS METAL COMPLEXES

Compound	TG range (°C)	DTG_{Max} (°C)	Mass loss (%)	Assignment	Residue	DSC (°C)
(HMePAI) = HL $C_{10}H_{10}N_4O$	25-116	286	1.75	Evolution of Co_2 and moisture	–	451 (+) 532 (+)
	116-297	450	15.79	Loss CH_3 group		
	297-431	521	31.58	Loss OH group		
	431-512		57.35	Loss azo group and		
	512'586		88.60	Loss imidazole ring		
				A part of the ligand		
$[Cr(C_{10}H_9N_4O)_2].Cl$	35-159	210	2.96	Evolution of Co_2 and moisture	Cr	507 (+) 548 (+)
	159-233	481	15.65	Loss CH_3 group		
	233-442	539	31.08	Loss azo group		
	442'576		89.77	Loss imidazole ring and		
				Loss of a part of the ligand		
$[Mn(C_{10}H_9N_4O)_2]$	34-160	493	3.33	Evolution of Co_2 and moisture	Mn	497 (+) 537 (+)
	160-312	532	21.29	Loss CH_3 group		
	312'465		33.90	Loss azo group		
	465-568		83.00	Loss imidazole ring and		
				Loss of a part of the ligand		
$[Fe(C_{10}H_9N_4O)_2].Cl$	36-131	202	2.35	Evolution of Co_2 and moisture	Fe	371 (+) 458 (+)
	131-224	363	51.08	Loss CH_3 group		
	224-338	450	28.75	Loss azo group		
	338-494		83.61	Loss imidazole ring and		
				Loss of a part of the ligand		
$[Co(C_{10}H_9N_4O)_2].Cl$	38-153	37	2.36	Evolution of Co_2 and moisture	Co	252 (-) 512 (+) 535 (+) 577 (+)
	153-231	252	15.69	Loss CH_3 group		
	231-448	536	34.21	Loss azo group		
	448-596	579	81.95	Loss imidazole ring and		
				Loss of a part of the ligand		
$[Ni(C_{10}H_9N_4O)_2]$	33-160	492	2.98	Evolution of Co_2 and moisture	Ni	493 (+) 592 (+)
	160-235	591	15.64	Loss CH_3 group		
	235-441		31.00	Loss azo group		
	441-578		89.78	Loss imidazole ring and		
				Loss of a part of the ligand		
$[Cu(C_{10}H_9N_4O)_2]$	36-163	217	3.32	Evolution of Co_2 and moisture	Cu	312 (+) 508 (+)
	163-315	309	21.31	Loss CH_3 group		
	315-463	502	34.02	Loss azo group		
	463-567		82.85	Loss imidazole ring and		
				Loss of a part of the ligand		
$[Zn(C_{10}H_9N_4O)_2]$	37-133	193	2.34	Evolution of Co_2 and moisture	Zn	386 (+) 474 (+)
	133-226	387	15.06	Loss CH_3 group		
	226-339	462	28.73	Loss azo group		
	339-493	469	83.63	Loss imidazole ring and		
				Loss of a part of the ligand		
$[Cd(C_{10}H_9N_4O)_2]$	36-155	213	2.33	Evolution of Co_2 and moisture	Cd	422 (+) 545(+)
	155-229	421	15.73	Loss CH_3 group		
	229-446	534	34.18	Loss azo group		
	446-598		82.01	Loss imidazole ring and		
				Loss of a part of the ligand		
$[Hg(C_{10}H_9N_4O)_2]$	36-161	467	2.95	Evolution of Co_2 and moisture	Hg	470 (+) 537(+)
	161-231	533	15.67	Loss CH_3 group		
	231-444	619	31.06	Loss azo group		
	444-574		89.76	Loss imidazole ring and		
				Loss of a part of the ligand		

TABLE-6
INTER PLANAR DISTANCES AND THE 2θ VALUE OF EACH PEAK, RELATIVE INTENSITY, CRYSTALLOGRAPHIC DATA AND FWHM FOR LIGAND (HMePAI) AND METAL COMPLEXES

Compound	$2\theta_{obs}$ (°)	d_{obs} spacing (Å)	Intensity (I/I_o) (%)	Pos. [2θ, °]	FWHM [2θ, °]	Crystallite size (D, nm)	Lattice strain
HL= HMePAI	27.5	3.2413	19	27.5869	0.1771	48.26	0.0031
	32.0	2.7946	100	31.8806	0.2362	36.55	0.0036
	45.5	1.9919	40	45.6412	0.1771	50.85	0.0018
	54.0	1.6967	6	54.0206	0.2362	39.44	0.0020
	56.5	1.6274	15	56.6248	0.2362	39.92	0.0019
	66.5	1.4049	12	66.3400	0.3542	27.99	0.0024
	73.25	1.2912	2	73.1937	0.1771	58.37	0.0010
	75.5	1.2582	14	75.3998	0.2880	36.42	0.0016

	21.25	4.1778	31	27.4319	0.3542	24.12	0.0063
	28.0	3.1841	31	31.7620	0.2362	36.54	0.0036
	32.0	2.7946	100	45.5145	0.1771	50.83	0.0018
$[Cr(C_{10}H_9N_4O)_2].Cl$	45.5	1.9919	38	56.5346	0.2362	39.9	0.0019
	56.5	1.6274	17	66.2849	0.3542	27.99	0.0024
	66.5	1.4049	8	75.3267	0.3600	29.12	0.0020
	75.5	1.2582	11				
	23.5	3.7826	65	31.8420	0.1771	48.74	0.0027
	32.0	2.7946	100	45.5842	0.2362	38.12	0.0025
	46.0	1.9714	56	56.5969	0.2952	31.93	0.0024
$[Mn(C_{10}H_9N_4O)_2]$	57.0	1.6143	31	75.4764	0.4320	24.29	0.0024
	59.5	1.5523	21				
	66.5	1.4049	21				
	75.5	1.2582	23				
	21.5	4.1298	29	23.0329	0.1771	47.84	0.0038
	23.0	3.8637	34	27.4571	0.1771	48.25	0.0032
	27.5	3.2408	28	31.8039	0.2362	36.54	0.0036
	31.75	2.8160	100	32.7477	0.1771	48.85	0.0026
	32.75	2.7323	55	45.5547	0.2362	38.11	0.0025
	40.25	2.2388	13	46.9529	0.1771	51.10	0.0018
$[Fe(C_{10}H_9N_4O)_2].Cl$	45.5	1.9919	53	56.5666	0.2362	39.90	0.0019
	47.0	1.9318	16	58.3699	0.2952	32.21	0.0023
	53.0	1.7264	11	66.3066	0.2362	41.97	0.0016
	56.5	1.6274	17	75.3659	0.2880	36.41	0.0016
	58.5	1.5765	12				
	66.5	1.4049	9				
	68.5	1.3687	8				
	75.5	1.2582	14				
	23.5	3.7826	97	31.8958	0.1771	48.75	0.0027
	32.5	2.7527	100	45.6464	0.2362	38.13	0.0024
	46.0	1.9714	71	56.6933	0.4320	21.83	0.0035
$[Co(C_{10}H_9N_4O)_2].Cl$	57.0	1.6143	36				
	67.0	1.3956	29				
	75.5	1.2582	27				
	76.75	1.2408	24				
	21.75	4.0828	100	31.7813	0.2362	36.54	0.0036
	32.0	2.7946	88	45.5279	0.2160	41.68	0.0022
$[Ni(C_{10}H_9N_4O)_2]$	46.5	1.9514	51				
	57.0	1.6143	30				
	75.5	1.2582	22				
	22.75	3.9056	64	31.9043	0.1771	48.75	0.0027
	32.0	2.7946	100	45.6348	0.2362	38.13	0.0024
	46.0	1.9714	57	56.6501	0.3542	26.62	0.0029
$[Cu(C_{10}H_9N_4O)_2]$	56.75	1.6209	31	75.4511	0.4320	24.29	0.0024
	66.75	1.4002	27				
	70.25	1.3388	24				
	75.5	1.2582	25				
	22.0	4.0370	72	31.8421	0.1771	48.74	0.0027
	31.75	2.8160	100	45.5741	0.1771	50.84	0.0018
	42.25	2.1373	31	56.6119	0.2952	31.94	0.0024
$[Zn(C_{10}H_9N_4O)_2]$	45.5	1.9919	73	75.4110	0.4320	24.28	0.0024
	56.75	1.6209	28				
	66.5	1.4049	19				
	75.5	1.2582	19				
	24.25	3.6673	44	31. 9590	0.2952	29.25	0.0045
	32.0	2.7946	100	34.1917	0.4723	18.39	0.0067
	34.25	2.6160	35	45.6891	0.2952	30.51	0.0031
$[Cd(C_{10}H_9N_4O)_2]$	45.75	1.9816	61	56.7272	0.2952	31.95	0.0024
	56.75	1.6209	27	66.4988	0.7085	14.01	0.0047
	66.5	1.4049	19	75.5104	0.3600	29.16	0.0020
	75.5	1.2582	24				
	23.25	3.8227	100	31.8700	0.2362	36.55	0.0036
	32.25	2.7735	84	45.6097	0.3600	25.01	0.0037
	41.75	2.1618	42				
$[Hg(C_{10}H_9N_4O)_2]$	45.75	1.9816	52				
	56.75	1.6209	30				
	59.25	1.5583	26				
	75.5	1.2582	21				

angle and full width at half maximum of an observed peak, respectively [58-60].

SEM analysis: The properties of ligand and its metal complexes like surface morphology, distribution of particles, aggregation and shape of the particles study by scanning electron microscopy (SEM) technique. SEM image (Fig. 5) shows that the ligand (HMePAI) has form of peripheral spherical shape with average size 85 nm with a ratio of less than aggregation. The SEM of the complexes revealed that the particles are agglomerated and non-uniform particles are observed in some cases. Moreover, SEM micrographs of the metal complexes revealed that the surface morphology of metal complexes is changed by changing the metal ions [61,62]. The calculations of particles size were performed using MagniSci software (Fig. 5). The SEM image of Cr(III) complex seemed heterogeneous surfaced type average particle size175 nm. The SEM analysis of Mn(II) complex appeared in the form of heterogeneous the surface with average particle size 145 nm. The SEM image of Fe(III) complex appeared in the form of heterogeneous surface with average particle size of 155 nm. As the analysis of SEM

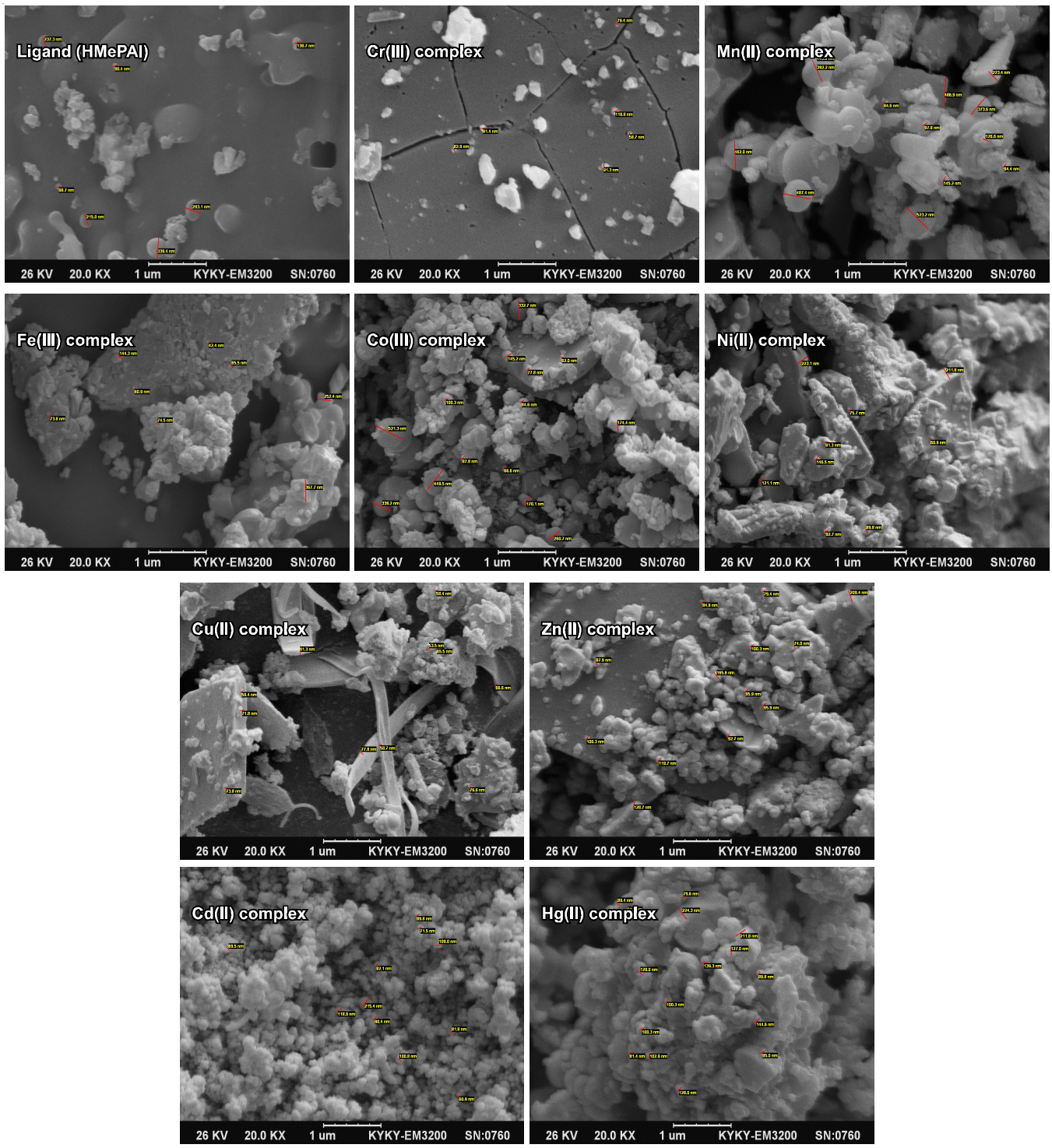

Fig. 5. SEM images of ligand (HMePAI)and prepared metal complexes

for Co(III) complex seemed heterogeneous surfaced type with average size of 120 nm. The SEM image for Ni(II) complex appeared in the form of a small particle size is heterogeneous surface and the average particle size of150 nm, either the analysis of SEM for Cu(II) appeared in the form of heterogeneous surface and the average particle size 160 nm. The SEM image of Zn(II) complex seemed heterogeneous surfaced with average particle size 150 nm. The analysis of SEM for complex Cd(II) complex appeared in the form of small particles size heterogeneous surface and the average particle size of 130 nm. The SEM image of Hg(II) seemed heterogeneous surfaced type with average particle size 125 nm.

Anitbacterial activity: The antibacterial activity of azo dye ligand (HMePAI) and its metal complexes have been tested for *in vitro* growth inhibitory activity against Gram-positive bacteria: *Staphylococcus aureus*, Gram-negative bacteria: *Escherichia coli* by using spots diffusion method. All of tested ligand and its metal complexes show a remarkable antibacterial activity against tested bacteria (Table-7). The *Staphylococcus aureus* bacteria was of a high activity and sensitivity towards ligand and all metal complexes except the Cu(II), Zn(II) and Hg(II) complexes which were resistant and inactive while *Escherichia coli* bacteria which was inactive and not sensitive towards ligand and all metal complexes. The mechanism of action of antibacterial drug can be discussed under four headings: (1): inhibition of cell wall, (2): inhibition of cell membrane function, (3): inhibition of protein prepared and (4): inhibition of nucleic acid [29,63].

Cell viability and cytotoxicity assays: The lines of cancerous liver cells of the type $HePG_2$ are used and compared with line of the ordinary cells. These lines are procured from department of pharmacology/faculty of medicine center for natural product research and drug discovery/University of Malya, Kualalampur, Malaysia. Freshney method is used for the development of the cell of cancerous cell line of the liver $HePG_2$. The data is statistically analyzed by a one way analysis of variance ANOVA (Duncan) was performed to test whether group variance was significant or not. Data were expressed as mean ± standard error and statistical significances were carried out using SPSS program version 20 and drowned using Graph Pad Prism version 6. The relation between the biological activity of the cancerous line cell of the liver $HePG_2$ and normal line cells of the liver WRL and the concentration of the ligand and its complex with Ni(II) ion. It is observed that the inhibition of the ligand (HMePAI) differs with difference of cell line where the number of the remaining living cells after the reaction with Ni(II) complex is about (99.62'47.07) % for the cancerous cell line of the liver $HePG_2$ and (99.57-90.86) % for normal cell line WRL. It is observed that the highest ratio of the inhibition of the ligand for the cancerous cell line of the liver $HePG_2$ is 47.07 % whereas the ratio of the normal cell line WRL is 99.86 % for the living cells and this indicates that Ni(II) complex has a higher efficiency than the ligand inhibiting the growth of cancerous cells. The reason behind this inhibition of the growth of cancer cell is that the ligand and Ni(II) complex include imidazole ring which has a high efficiency in inhibiting or stopping the growth of cancer cells. Moreover, increasing the efficiency in inhibiting the growth of cancer cells by using Ni(II) complex is more than that in the ligand because it includes two imidazole rings. These kind of imidazole compounds are used in treating blood cancer, lung cancer, hepatomegaly and breast cancer [64,65].

The results show also that the type of compound and its concentration has an essential role in determining the ratio of inhibiting the growth of cancer cells depending on the dose which increases the inhibition by increasing the concentration to certain limits where the lesser the concentration the material, the easier it is to penetrate the outer membrane of the cells, but not to limit the dilution which loses its effectiveness.

Also it has been found through the tests conducted on ligand and its complex with Ni(II) ion to know inhibition concentration IC_{50}, that in case of using ligand, it kills half of infected cells and its effect will be lesser on the non-infected cells because it needs high concentration for its half to be killed, *i.e.* it is about four times of the concentration required to kill cancerous cells. In case of Ni(II) complex, it is observed that IC_{50} is not within concentration used and this can be considered an excellent result, the Ni(II) complex kills the cancerous cells and its effect is imperceptible on the normal cells because they need very high concentration in order for their half to be killed where it reaches approximately three hundred times required to kill half of the cancerous cells. This is an important and new result in our study. Table-8 show the results mentioned above. Through assays conducted to identify the possibility of using the ligand (HMePAI) and Ni(II) complex anticancer drugs.

Conclusion

In the present study, the synthesis, spectral and thermal analyses of Cr(III), Mn(II), Fe(III), Co(III), Ni(II), Cu(II), Zn(II), Cd(II) and Hg(II) complexes of aryl azo imidazole ligand (HMePAI) have been carried out. The azo dye ligand (HMePAI) acts as neutral tridentate coordinating through phenolic oxygen, nitrogen of azo group (N_3) which is the farthest of imidazole ring and nitrogen of imidazole ring (N3) to form two five membered metal rings. On the basis of their analytical and spectral data, we propose octahedral geometry for metal complexes. The ligand and its metal complexes different morphologies as appeared in XRD and SEM studies. The ligand and its metal complexes are found to have higher biological activities. Also, the study of ligand and Ni(II)-complex in cells viability and cytotoxicity assays by using the lines of cancerous liver cells, of the type HePG2 and compared with line of the

TABLE-7
ANTIBACTERIAL ACTIVITY DATA (ZONE OF INHIBITION IN mm) OF AZO DYE LIGAND (HMePAI) AND ITS METAL COMPLEXES

Compounds	HMePAI	Cr(III)	Mn(II)	Fe(III)	Co(III)	Ni(II)	Cu(II)	Zn(II)	Cd(II)	Hg(II)
S. aureus	+++ 21 mm	+++ 16.5 mm	+++ 15.5 mm	+++ 15.0 mm	+++ 17 mm	+++ 17.5 mm	– 0 mm	– 0 mm	+++ 17 mm	– 0 mm
E. coli	–	–	–	–	–	–	–	–	–+	–

Note: Highly active = +++ Inhibition zone > 12 mm

TABLE-8
RELATION BETWEEN INHIBITION CONCENTRATION (IC_{50}) AND CELL VIABILITY/CYTOTOXICITY FOR LIGAND (HMePAI) AND Ni(II) COMPLEX

S. No.	Non-linear fitting	Ligand (HMePAI)		Ni(II) complex	
		Cancerous line cells of liver $HePG_2$	Normal line cells of liver WRL	Cancerous line cells of liver $HePG_2$	Normal line cells of liver WRL
1	log (inhibitor) *vs*. response (three parameters)				Ambiguous
2	Best-fit values				
3	Bottom	-30.76	-4.703	-25.55	~ -2426
4	Top	112.2	101.5	107.3	98.17
5	Log IC_{50}	2.477	3.092	2.678	~5.154
6	IC_{50}	299.9	1236	476.2	~142711
7	Span	143.0	106.2	132.8	~2524
8	Std. Error				
9	Bottom	17.38	192.7	25.56	~1.449e+006
10	Top	3.433	3.380	2.396	2.259
11	Log IC_{50}	0.1213	1.057	0.1544	~250.0
12	Span	15.08	190.2	23.86	~1.449e+006
13	95 % confidence Intervals				
14	Bottom	-105.5 to 44.02	-833.9 to 824.5	-135.5 to 84.44	(Very wide)
15	Top	97.44 to 127.0	86.96 to 116.0	96.97 to 117.6	88.45 to 107.9
16	Log IC_{50}	1.955 to 2.999	-1.454 to 7.638	2.013 to 3.342	(Very wide)
17	IC_{50}	90.16 to 997.4	0.03512 to 4.348×10^{7}	103.1 to 2199	(Very wide)
18	Span	78.08 to 207.9	-712.2 to 924.6	30.14 to 235.5	(Very wide)
19	Goodness of fit				
20	Degrees of freedom	2	2	2	2
21	R square	0.9970	0.9566	0.9967	0.7561
22	Absolute Sum of Square	9.832	16.96	6.257	9.329
23	Sy.x	2.217	2.912	1.769	2.160
25	Number of points				
26	Analyzed	5	5	5	5

ordinary cells, through tests conducted to identify the possibility of using the ligand and Ni(II)-complex anticancer drug.

REFERENCES

1. P.M. Savanor, S.K. Bhat and R.N. Tantry, *Res. J. Chem. Sci.*, **3**, 38 (2013).
2. A. Khosravi, S. Moradian, K. Gharaning and F.A. Taromi *Dyes Pigments*, **69**, 79 (2006); https://doi.org/10.1016/j.dyepig.2005.02.007.
3. Y.K. Gupta and S. Agarwal, *Res. J. Chem. Sci.*, **2**, 68 (2012).
4. D.R. Waring and G. Hallas, The Chemistry and Application of Dyes, Plenum Press, New York and London (1990).
5. M.S. Bashandy, F.A. Mohamed, M.M. El-Molla, M.B. Sheier and A.H. Bedair, *Open J. Med. Chem.*, **6**, 18 (2016); https://doi.org/10.4236/ojmc.2016.61002.
6. K.J. Al-Adilee and H.K. Dakhil, *J. Al-Qadisiya Pure Sci.*, **16**, 94 (2011).
7. K. Komatsu and N. Kuroki, *J. Soc. Chem. Ind. Jpn.*, **73**, 2190 (1970); https://doi.org/10.1246/nikkashi1898.73.10_2190.
8. M. Hranjec, K. Starcevic, S.K. Pavelic, P. Lucin, K. Pavelic and G.K. Zamola, *Eur. J. Med. Chem.*, **46**, 2274 (2011); https://doi.org/10.1016/j.ejmech.2011.03.008.
9. M. Hranjec, G. Pavlovic and G.K. Zamola, *J. Mol. Struct.*, **1007**, 242 (2012); https://doi.org/10.1016/j.molstruc.2011.10.054.
10. K.F. Ansari and C. Lal, *Eur. J. Med. Chem.*, **44**, 4028 (2009); https://doi.org/10.1016/j.ejmech.2009.04.037.
11. N.S. Pawar, D.S. Dalal, S.R. Shimpi and P.P. Mahulikar, *Eur. J. Pharm. Sci.*, **21**, 115 (2004); https://doi.org/10.1016/j.ejps.2003.09.001.
12. A. Mohammadi, B. Khalili and M. Tahavor, *Spectrochim. Acta A Mol. Biomol. Spectrosc.*, **150**, 799 (2015); https://doi.org/10.1016/j.saa.2015.06.024.
13. K. Kubo, Y. Kohara, Y. Yoshimura, Y. Inada, Y. Shibouta, Y. Furukawa, T. Kato, K. Nishikawa and T. Naka, *J. Med. Chem.*, **36**, 2343 (1993); https://doi.org/10.1021/jm00068a011.
14. W.W.K.R. Mederski, D. Dorsch, S. Anzali, J. Gleitz, B. Cezanne and C. Tsaklakidis, *Bioorg. Med. Chem. Lett.*, **14**, 3763 (2004); https://doi.org/10.1016/j.bmcl.2004.04.097.
15. H. Park, E.-R. Kim, D.J. Kim and H. Lee, *Bull. Chem. Soc. Jpn.*, **75**, 2067 (2002); https://doi.org/10.1246/bcsj.75.2067.
16. K.I. Birkett and P. Gregory, *Dyes Pigments*, **7**, 341 (1986); https://doi.org/10.1016/0143-7208(86)80002-X.
17. R.H. Sprague, US Patent 289238 (1959).
18. I.Q. Prager and R.H. Sprague, Photographic Sensitizing Dyes Derived from 2-Alkyl-5,6-dihydro-4*H*-pyrano(3, 2d) thiazole, US Patent 2886565 (1959).
19. K. Bredereck, *Dyes Pigments*, **21**, 23 (1993); https://doi.org/10.1016/0143-7208(93)85003-I.
20. G.M. Malik and S.K. Zadafiya, *Der Chem. Sinica*, **1**, 15 (2010).
21. H. Teranishi, K. Takagawa, Y. Arai, K. Wakaki, Y. Sumi and K. Takaya, *J. Occup. Health*, **44**, 60 (2002); https://doi.org/10.1539/joh.44.60.
22. A. Nandi, C. Sen, D. Mallick, R.K. Sinha and C. Sinha, *Adv. Mater. Phys. Chem.*, **3**, 133 (2013); https://doi.org/10.4236/ampc.2013.32019.
23. K.J. Al-Adilee, *Asian J. Chem.*, **24**, 5597 (2012).
24. K.J. Al-Adilee, H.A. Habeeb and M.N. Dawood, *Res. J. Pharma. Bio. Chem. Sci.*, **7**, 2882 (2016).
25. A.I. Vogel, A Text Book of Quantitative Inorganic Analysis, Longman ELBS, London, edn 3 (1968).
26. K.J. Al-Adilee, *Res. J. Pharm. Bio. Chem. Sci.*, **6**, 1297 (2015).
27. K.J. Al-Adilee, K.A. Abedalrazaq and Z.M. Al-Hamdiny, *Asian J. Chem.*, **25**, 10475 (2013); https://doi.org/10.14233/ajchem.2013.15735.
28. K.J. Al-Adilee and D.Y. Fanfon, *J. Chem. Chem. Eng.*, **6**, 1016 (2012); https://doi.org/10.17265/1934-7375/2012.11.011.
29. J.Z. Mohammed, H. Abbas and A.A.M. Ali, *Int. J. Curr. Res.*, **5**, 3705 (2013).
30. H. Irving and R.J.P. Williams, *J. Chem. Soc.*, 3192 (1953); https://doi.org/10.1039/jr9530003192.
31. K.J. Al-Adilee, *Iraqi Nat. J. Chem. J. Chem.*, **28**, 585 (2007).

32. M.B. Halli, K. Mallikarjun and S. Sadusuryakant, *J. Chem. Pharm. Res.*, **7**, 1797 (2015).
33. K.J. Al-Adilee and H.A.K. Kyhoiesh, *J. Mol. Struct.*, 1137, 160 (2017); https://doi.org/10.1016/j.molstruc.2017.01.054.
34. M. Ozkutuk, E. Ipek, B. Aydiner, S. Mamas and Z. Seferoglu, *J. Mol. Struct.*, **1108**, 521 (2016); https://doi.org/10.1016/j.molstruc.2015.12.032.
35. K.J. Al-Adilee and B.A. Hatam, *J. Adv. Chem.*, **3**, 3412 (2015).
36. A.A. El-Bindary, G.G. Mohamed, A.Z. El-Sonbati, M.A. Diab, W.M.I. Hassan, Sh.M. Morgan and A.K.Elkholy, *J. Mol. Liq*., **218**, 138 (2016); https://doi.org/10.1016/j.molliq.2016.02.021.
37. R. Mahmoud, A.M. Hammam, S.A. El-Gyar and S.A. Ibrahim, *Monatsh. Chem.*, **117**, 313 (1986); https://doi.org/10.1007/BF00816525.
38. Y. Yildiz, M.K. M. Keles, A.K. A. Kaya and S.D. S. Dincer, *Chem. Sci. Trans.*, **2**, 547 (2013); https://doi.org/10.7598/cst2013.353.
39. S. Saha, T. Majumdar and Mahapatra, *Transition Met. Chem*, **31**, 1017 (2006); https://doi.org/10.1007/s11243-006-0101-6.
40. S. Chandra, M. Tyagi and K. Sharma, *J. Iran. Chem. Soc.*, **6**, 310 (2009); https://doi.org/10.1007/BF03245839.
41. L. Mangsup, S. Siripaisarnpipat and N. Chaichit, *Anal. Sci.*, **19**, 1345 (2003); https://doi.org/10.2116/analsci.19.1345.
42. K. Dey and K.K. Nandi, *Indian J. Chem.*, **35A**, 766 (1996).
43. J. C. Bailer, H. Emeleus and R. Nypholm, Comprehensive Inorganic Chemistry, Pergamon Press (1973).
44. S. Rao and K.H. Reddy, *Indian J. Chem.*, **35A**, 681 (1996).
45. T.K. Pal and C. Sinha, *Proc. Indiana Acad. Sci.*, **113**, 173 (2001); https://doi.org/10.1007/BF02704067.
46. O. Yamauchi, *Talanta*, **15**, 177 (1968); https://doi.org/10.1016/0039-9140(68)80220-6.
47. B.B. Mahapatra and S.K. Pujari, *Transition Met. Chem.*, **8**, 202 (1983); https://doi.org/10.1007/BF00620688.
48. C.J. Ballhausen, Introduction to Ligand Field Theory, McGraw-Hill, New York (1962).
49. M. Kurahashi, *Bull. Chem. Soc. Jpn.*, **47**, 2067 (1974); https://doi.org/10.1246/bcsj.47.2067.
50. P.K. Ghosh, S. Saha and A. Mahapatra, *Chem. Cent. J.*, **1**, 23 (2007); https://doi.org/10.1186/1752-153X-1-23.
51. G. Valamary and R. Subbalaksmi, *Indian J. Appl. Res.*, **3**, 43 (2013).
52. R.L. Dutta and A. Syamal, Elements of Magneto Chemistry, Affiliated East West Press, New Delhi, p. 101 (1993).
53. E. Helen, P. Bai and S. Vairam, *Asian J. Chem.*, **25**, 209 (2013); https://doi.org/10.14233/ajchem.2013.12895.
54. M. Arshad, Saeed-ur-Rehman, A.H. Qureshi, K. Masud, M. Arif, A. Saeed and R. Ahmed, *Turk. J. Chem.*, **32**, 593 (2008).
55. E.T.G. Cavalheiro, F.C.D. Lemos, J.Z. Schpector and E.R. Dockal, *Thermochim. Acta*, **370**, 129 (2001); https://doi.org/10.1016/S0040-6031(00)00777-2.
56. I. Kolthoff, Treatise of Analytical Chemistry, Interscience, New York, Part I, pp 745 (1959).
57. Powder Diffraction file, Inorganic, Published by the Joint Committee on Powder Diffraction Standard, vol. 1,No. PDIS 10Irb:662 (1967).
58. V.S. Gavhane, A.S. Rajbhoj and S.T. Gaikwad, *Pharmachem.*, **8**, 275 (2016).
59. R.M.A.Q. Jamhour, *Can. Chem. Trans.*, **2**, 306 (2014); https://doi.org/10.13179/canchemtrans.2014.02.03.0111.
60. M.I. Abou-Dobara, A.Z. El-Sonbati, M.A. Diab, A.A. El-Bindary and S.M. Morgan, *J. Microb. Biochem. Technol.*, **S3**, 06 (2014); https://doi.org/10.4172/1948-5948.S3-006.
61. M. Montazerozohori, S.M. Jahromi and A. Naghiha, *J. Ind. Eng. Chem.*, **22**, 248 (2014); https://doi.org/10.1016/j.jiec.2014.07.017.
62. M. Shakir, S. Hanif, M.A. Sherwani, O. Mohammad and S.I. Al-Resayes, *J. Mol. Struct.*, **1092**, 143 (2015); https://doi.org/10.1016/j.molstruc.2015.03.012.
63. E. Jawetz, J.L. Melnick and E.A. Adelbrerg, Medical Microbiology, McGraw Hill, USA, edn 24 (2007).
64. F. Bellina, S. Cauteruccio, A. Di Fiore and R. Rossi, *Eur. J. Org. Chem.*, **2008**, 5436 (2008); https://doi.org/10.1002/ejoc.200800738.
65. F. Li, J. Cui, L. Guo, X. Qian, W. Ren, K. Wang and F. Liu, *Bioorg. Med. Chem.*, **15**, 5114 (2007); https://doi.org/10.1016/j.bmc.2007.05.032.